

# Dynamical formation of domains in net-baryon density at the QCD phase transition

Christoph Herold,<sup>1,2</sup> Marlene Nahrgang,<sup>2,3</sup> Igor Mishustin,<sup>2,4</sup> and Marcus Bleicher<sup>1,2</sup>

<sup>1</sup>*Institut für Theoretische Physik, Goethe-Universität,  
Max-von-Laue-Strasse 1, 60438 Frankfurt am Main, Germany*

<sup>2</sup>*Frankfurt Institute for Advanced Studies (FIAS),  
Ruth-Moufang-Strasse 1, 60438 Frankfurt am Main, Germany*

<sup>3</sup>*SUBATECH, Université de Nantes, EMN, IN2P3/CNRS,  
4 rue Alfred Kastler, 44307 Nantes cedex 3, France*

<sup>4</sup>*Kurchatov Institute, National Research Center, 123182 Moscow, Russia*

(Dated: April 20, 2019)

We consider the (3+1) dimensional expansion and cooling of the chirally-restored and deconfined matter at finite net-baryon densities as created in heavy-ion collisions. In our approach, chiral fields and the Polyakov loop propagate explicitly within a medium represented by a quark-antiquark fluid. The interaction between the fields and the fluid leads to dissipation and noise, which in turn affect the field fluctuations. For the first time in a realistic dynamical study, we demonstrate the possibility of domain formation in a first-order phase transition of QCD matter.

PACS numbers: 25.75.q, 47.75.+f, 11.30.Qc, 24.60.Ky

The investigation of phase transitions in strongly-interacting matter during a heavy-ion collision is necessarily accompanied by nonequilibrium phenomena due to the fast collective expansion. At a first-order phase transition, which is suggested by effective models of QCD at large baryochemical potentials  $\mu_B$  [1, 2], the rapid dynamics should lead to strong supercooling. If nucleation times are large, a fast cooling will drive the system into the spinodal region, where the metastable state will decay via spinodal decomposition. This can lead to the formation of domains of the decaying phase embedded in the low-density background [3–6]. Since at small baryochemical potentials lattice QCD calculations predict a crossover transition [7, 8], one may expect the first-order phase transition only at high values of  $\mu_B$  starting from a critical end point (CEP).

As the regime of high net-baryon densities will be accessible in future experiments at FAIR [9] and NICA [10], we will have the opportunity to directly investigate the first-order phase transition by looking for potential signals stemming from the spinodal dynamics.

In this letter we present a fully dynamical approach to the formation of domains at the first-order phase transition during a heavy-ion collision. For this purpose we apply the recently developed model of nonequilibrium (Polyakov-) chiral fluid dynamics (N $\chi$ FD, NP $\chi$ FD) [11–14], which extends earlier versions of chiral fluid dynamics [15, 16]. Here, the dynamics of the order parameter fields and their respective fluctuations are described by a stochastic Langevin equation coupled to the fluid dynamical expansion of the bulk matter. We adopt the Polyakov-Quark-Meson (PQM) model, which exhibits the expected thermodynamic phase structure of QCD at mean-field level [2] and beyond [17].

In the PQM model the mesonic fields  $\sigma$  and  $\vec{\pi}$  couple to the quarks and antiquarks with a coupling strength  $g$ .

The temporal component of the color gauge field also couples to the quarks, generating the Polyakov loop  $\ell$  in the mean-field effective Potential  $V_{\text{eff}}$  which is represented as

$$V_{\text{eff}} = U(\sigma) + \mathcal{U}(\ell, T) + \Omega_{\text{q}\bar{\text{q}}}(\sigma, \ell, T, \mu) . \quad (1)$$

Here,  $U$  is the classical Mexican hat potential of the mesonic fields,  $\mathcal{U}$  is a temperature-dependent effective potential of the Polyakov loop [2, 18, 19] and the mean-field thermodynamic potential of the quarks reads

$$\Omega_{\text{q}\bar{\text{q}}} = - 2N_f T \int \frac{d^3p}{(2\pi)^3} \left\{ (\ln [g^{(+)}(\sigma, \ell, T, \mu)]) + \ln [g^{(-)}(\sigma, \ell, T, \mu)] \right\} . \quad (2)$$

We used the abbreviating notation

$$g^{(+)} = 1 + 3\ell e^{-E^{(+)} / T} + 3\ell e^{-2E^{(+)} / T} + e^{-3E^{(+)} / T} , \quad (3)$$

$$g^{(-)} = 1 + 3\ell e^{-E^{(-)} / T} + 3\ell e^{-2E^{(-)} / T} + e^{-3E^{(-)} / T} , \quad (4)$$

with the number of flavors  $N_f = 2$  and  $E^{(+)} = E_q - \mu$ ,  $E^{(-)} = E_q + \mu$ , where  $\mu = \mu_B / 3$  is the quark chemical potential. Throughout this work, we neglect pion fluctuations and concentrate on the sigma field and the Polyakov loop, which are the order parameters for the chiral and deconfinement transition. The energy of the quarks  $E_q = \sqrt{p^2 + m_q^2}$  depends on the sigma field via the dynamically generated effective mass  $m_q = g|\sigma|$ . In the mean-field approximation, the chiral and deconfinement transition coincide for all values of  $\mu$ . We also find a common CEP at  $(T_{\text{cp}}, \mu_{\text{cp}}) = (152, 160)$  MeV.

For effective models of the present type it was found in [20, 21] that nucleation times are much longer than typical expansion times of the fireball, which implies that the system will strongly supercool. This conclusion was

confirmed within the present model in [12, 14], thus giving us the reason to expect observable signals stemming from spinodal decomposition.

We now briefly describe the nonequilibrium Polyakov-chiral fluid dynamics model (NP $\chi$ FD). In this approach the sigma field is propagated according to a Langevin equation

$$\partial_\mu \partial^\mu \sigma + \eta_\sigma \partial_t \sigma + \frac{\delta V_{\text{eff}}}{\delta \sigma} = \xi_\sigma, \quad (5)$$

which besides the standard mean-field contribution contains the damping term with friction coefficient  $\eta_\sigma$  and the stochastic noise field  $\xi_\sigma$ . For  $m_\sigma(T) > 2m_q(T) = 2g\sigma_{\text{eq}}(T)$  the damping coefficient due to the decay of the zero mode sigma field into a quark-antiquark pair ( $\sigma \rightarrow q + \bar{q}$ ) is given by [11]

$$\eta_\sigma = \frac{12g^2}{\pi} \left[ 1 - 2n_F \left( \frac{m_\sigma}{2} \right) \right] \frac{1}{m_\sigma^2} \left( \frac{m_\sigma^2}{4} - m_q^2 \right)^{3/2}. \quad (6)$$

Since we are mainly interested in the long-range fluctuations of the sigma field, we use the damping coefficient (6) for all modes in the Langevin equation. At lower temperatures it vanishes because this decay is kinematically forbidden as  $m_\sigma(T) < 2m_q(T) = 2g\sigma_{\text{eq}}(T)$ . However, the sigma field is further damped due to interaction with the hard chiral modes [22, 23], which can be represented by the reaction  $\sigma \leftrightarrow 2\pi$ . To account for them we use the value  $\eta = 2.2/\text{fm}$  [24] for the kinematic range  $2m_q > m_\sigma(T) > 2m_\pi$ .

The stochastic field in the Langevin equation (5) is given by a Gaussian distribution with zero mean

$$\langle \xi_\sigma(t) \rangle_\xi = 0. \quad (7)$$

The amplitude of the noise is determined by the dissipation-fluctuation theorem

$$\langle \xi_\sigma(t, \vec{x}) \xi_\sigma(t', \vec{x}') \rangle_\xi = \delta(\vec{x} - \vec{x}') \delta(t - t') m_\sigma \eta_\sigma \coth \left( \frac{m_\sigma}{2T} \right). \quad (8)$$

The dynamics of the Polyakov loop  $\ell$  is described by the relaxation equation

$$\eta_\ell \partial_t \ell T^2 + \frac{\delta V_{\text{eff}}}{\delta \ell} = \xi_\ell, \quad (9)$$

with a constant damping coefficient  $\eta_\ell = 5/\text{fm}$ . This value can only be estimated very roughly, but the results are largely independent of its specific choice [14]. The stochastic noise  $\xi_\ell$  is assumed to be Gaussian, too, and we impose the dissipation-fluctuation relation [14]

$$\langle \xi_\ell(t, \vec{x}) \xi_\ell(t', \vec{x}') \rangle_\xi T^2 = \frac{1}{V} \delta(t - t') \delta(\vec{x} - \vec{x}') 2\eta_\ell T. \quad (10)$$

In our dynamical model, the expansion of the fireball is described according to energy-momentum and baryon number conservation equations

$$\partial_\mu T^{\mu\nu}(t, \vec{x}) = S^\nu(t, \vec{x}), \quad (11)$$

$$\partial_\mu N^\mu(t, \vec{x}) = 0, \quad (12)$$

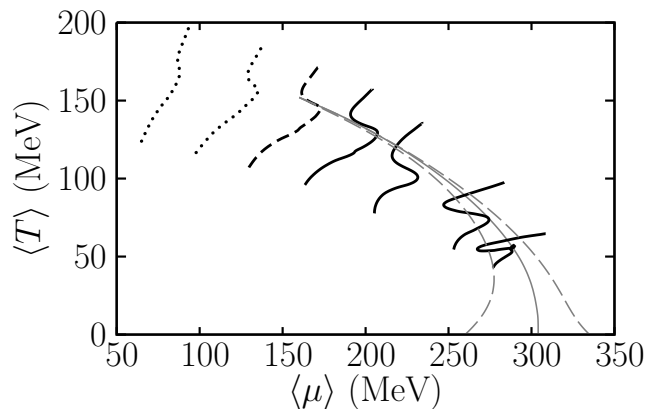


FIG. 1. Trajectories of the hydrodynamic simulation in the phase diagram for different initial conditions. Nonequilibrium effects lead to an overshooting of the first-order phase transition. The dashed grey lines denote the spinodal region.

where the source term  $S^\nu$  accounts for the energy-momentum exchange between the fluid and the fields. It is dominated by the energy dissipation from the sigma field and Polyakov loop to the fluid, controlled by the damping terms in Eqs. (5) and (9). This energy transfer is largest during the relaxation from the supercooled state.

Since the fields  $\sigma$  and  $\ell$  are not necessarily at their respective equilibrium values, the equation of state will depend explicitly on their local values  $\sigma(\vec{x})$ ,  $\ell(\vec{x})$ . This is different to standard fluid dynamical simulations using equilibrium equations of state. The corresponding equation of state of the fluid is obtained from the generalized thermodynamic relations

$$p(\sigma, \ell, T, \mu) = -\Omega_{\text{q}\bar{\text{q}}}, \quad (13)$$

$$e(\sigma, \ell, T, \mu) = T \frac{\partial p}{\partial T} + \mu \frac{\partial p}{\partial \mu} - p, \quad (14)$$

$$n(\sigma, \ell, T, \mu) = \frac{\partial p}{\partial \mu}. \quad (15)$$

where  $\sigma$  and  $\ell$  are functions of time and coordinates due to their own dynamics.

In the numerical implementation we solve the coupled equations (5), (9) and the (3+1) dimensional fluid dynamic equations (11), (12), as it is described in detail in [13, 14]. As initial states we consider spherical fireballs with various initial values of  $T$  and  $\mu$  to probe the crossover, CEP and first-order transitions. The order parameter fields are initialized in local thermal equilibrium for the initial  $T$ - $\mu$ -profiles.

The noise fields are sampled for each new time step according to the Gaussian distribution, given by Eqs. (8) and (10). For each grid cell ( $i \in 1 \dots N$ ) we average the initially uncorrelated noise variables over a surrounding volume  $V_\sigma^{\text{corr}} = 1/m_\sigma^3$  and  $V_\ell^{\text{corr}} = 1/m_\ell^3$  and attribute this average value to the noise in the respective grid cell

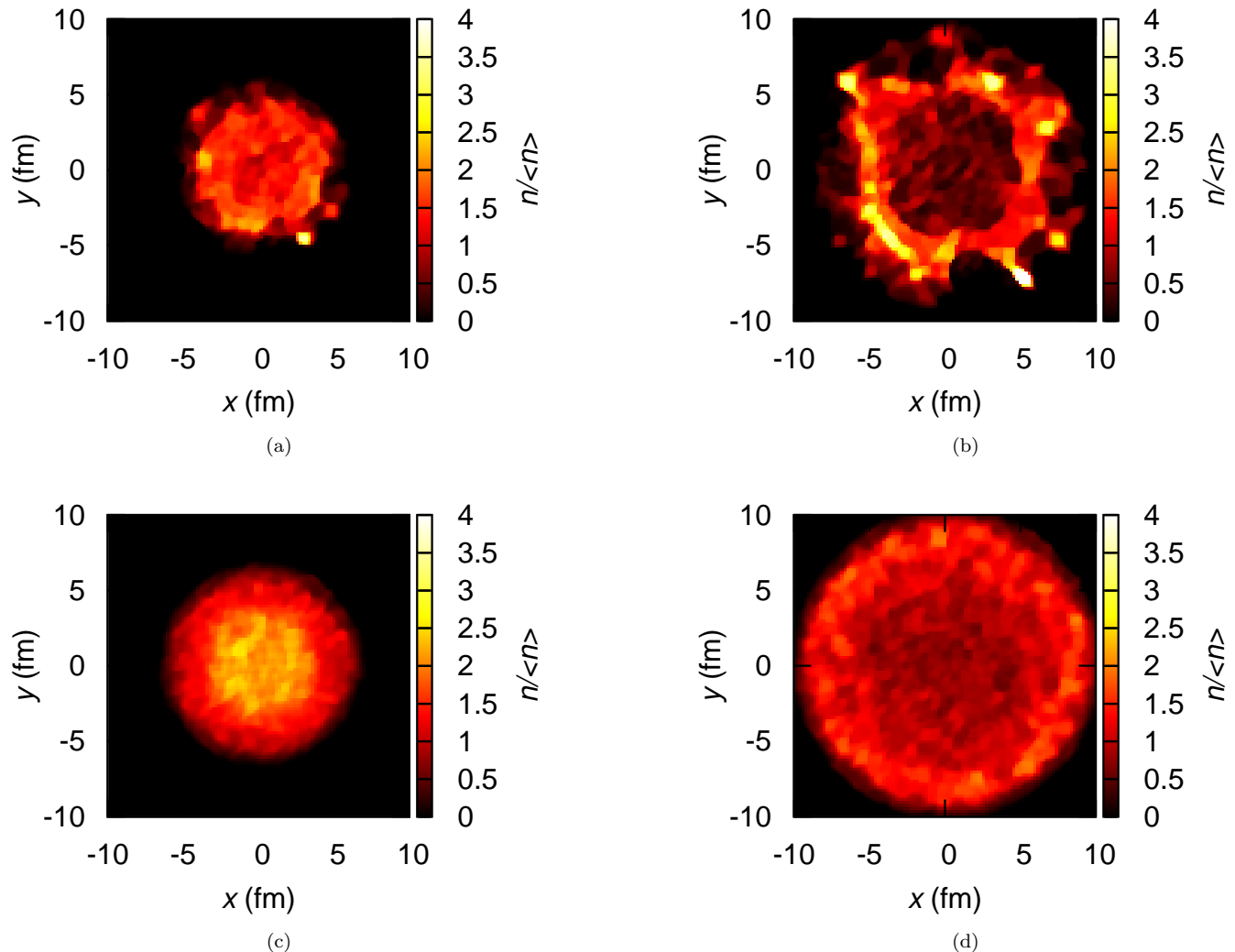


FIG. 2. (Color online) Relative net-baryon number density at  $z = 0$  for a first-order transition at  $t = 6$  fm (a) and  $t = 12$  fm (b) and for a transition through the CEP for  $t = 6$  fm (c) and  $t = 12$  fm (d). One can see that droplets of high density are formed at the first-order phase transition, while the density fluctuations remain small during an evolution through the CEP.

$i$ . Thus, the noise values in neighboring cells  $i$  and  $i + 1$ , which share large parts of the averaging volume, are correlated. This averaging reduces the variance of the noise and we need to recover the original local variance by rescaling. By this procedure we avoid an artificial correlation length equal to the cell spacing. In [14] we have found that during the simulation, the correlation length reaches values  $1.5 - 2.0$  fm around the CEP and remains small, at about  $0.2 - 0.4$  fm, in the case of a first-order transition.

The trajectories of the dynamic simulations in the  $T$ - $\mu$ -plane are presented in Fig. 1 together with the corresponding phase boundary and the spinodal lines. The averages  $\langle T \rangle$  and  $\langle \mu \rangle$  are calculated over a central box of  $1 \text{ fm}^3$ . The bending of the curves towards larger values of  $\mu$  is due to the rapid increase in the quark mass at the chiral transition. Similar behavior is already inherent in the

equilibrium isentropes, which follow the phase boundary towards larger  $\mu$  [1, 25]. In our dynamical simulations we see that at larger chemical potentials the bending only occurs after the trajectories have crossed the lower spinodal line. This behavior has a simple explanation: After crossing the first-order phase transition line, the system is still not able to overcome the potential barrier but gets trapped in a metastable chirally restored and deconfined state. After that barrier has vanished at the lower spinodal line, the system can roll down to the global minimum where the constituent quarks acquire their mass. As seen in Fig. 1, at highest  $\mu$ , one can observe a reheating of the quark fluid, an effect that we have already found in calculations at zero chemical potential [13, 14]. In summary we see that due to nonequilibrium effects the system supercools and spends an extended amount of time in the spinodal region. This may facilitate the

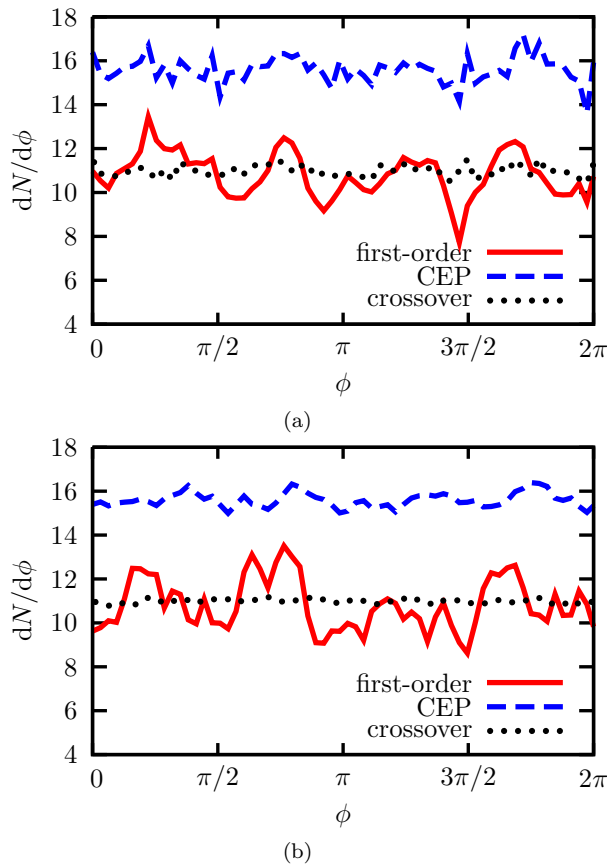


FIG. 3. (Color online) Azimuthal distribution of the baryon number density after  $t = 6$  fm (a) and  $t = 12$  fm (b) for several transition scenarios. We see that strong inhomogeneities develop at the first-order phase transition.

process of spinodal decomposition and therefore the development of interesting signals of the first-order phase transition.

In Fig. 2, we show two-dimensional maps (through the center of the fireball) of the relative net-baryon number density  $n/\langle n \rangle$ , for evolutions through both the first-order phase transition and the CEP. They correspond to the most right solid line and the dashed line in Fig. 1. Here,  $\langle n \rangle$  is the volume average over all cells with  $n > 0$ . We see that during the expansion the fluid evolves inhomogeneously in the case of a first-order transition, creating droplets of high baryon density at the periphery of the system. This effect is not observed at the CEP or crossover transition, where the spherical symmetry is preserved and no strong fluctuations occur.

It is clear that such inhomogeneities should lead to large fluctuations in the angular distribution of the net-baryon number  $dN/d\phi$ , where  $\phi$  is the azimuthal angle around the  $z$ -axis. Such distributions are shown in Fig. 3 for  $t = 6$  fm and  $t = 12$  fm. Here one can clearly see strong fluctuations of the net-baryon number as a function of  $\phi$  at the first-order transition in contrast to the CEP and crossover. One can notice the correlation of

bumps and deeps between the plots in Fig. 3 that indicates that the domains preserve their identity during this time interval. From Fig. 2 one can see that individual domains move radially outwards while their relative strength is amplified, since the system spends a long time in the spinodal region, see the corresponding trajectory in Fig. 1. From these figures we expect that after freeze-out the particles stemming from the domains will show a characteristic azimuthal spectrum leading to an enhancement of the higher flow harmonics.

In conclusion, we have demonstrated for the first time in a realistic dynamical study the formation of domains in net-baryon density at the first-order phase transition. These domains do not result from initial inhomogeneities but are due to the non-deterministic evolution of the system during spinodal decomposition. Within the setup of NP $\chi$ FD we have shown that a clear signal for a first-order phase transition can develop and survive during a realistic simulation of the expansion dynamics which is imprinted in net-baryon azimuthal fluctuations. These non-statistical fluctuations should be observed in single events. For a set of many events the prominent signature would be an enhancement of higher flow harmonics. By varying the beam energy one can get closer to the CEP where the signals of the first-order phase transition become weaker, until they finally cease. Being able to perform an energy scan, which covers small enough regions of  $\mu_B$ , would thus offer the possibility to discover and locate the CEP by looking where the signals of the first-order phase transition vanish.

The authors thank Stefan Leupold and Carsten Greiner for fruitful discussions and Dirk Rischke for providing the SHASTA code. This work was supported by the Hessian LOEWE initiative Helmholtz International Center for FAIR. I. M. acknowledges support from grant NSH-215.2012 2 (Russia).

- 
- [1] O. Scavenius, A. Mocsy, I. Mishustin, and D. Rischke, Phys.Rev. **C64**, 045202 (2001), arXiv:nucl-th/0007030 [nucl-th].
  - [2] B.-J. Schaefer, J. M. Pawłowski, and J. Wambach, Phys.Rev. **D76**, 074023 (2007), arXiv:0704.3234 [hep-ph].
  - [3] I. Mishustin, Phys.Rev.Lett. **82**, 4779 (1999), arXiv:hep-ph/9811307 [hep-ph].
  - [4] C. Sasaki, B. Friman, and K. Redlich, Phys.Rev. **D77**, 034024 (2008), arXiv:0712.2761 [hep-ph].
  - [5] J. Randrup, Phys.Rev. **C82**, 034902 (2010), arXiv:1007.1448 [nucl-th].
  - [6] J. Steinheimer and J. Randrup, Phys.Rev.Lett. **109**, 212301 (2012), arXiv:1209.2462 [nucl-th].
  - [7] S. Borsanyi *et al.* (Wuppertal-Budapest Collaboration), JHEP **1009**, 073 (2010), arXiv:1005.3508 [hep-lat].

- [8] W. Soldner (HotQCD collaboration), PoS **LAT-TICE2010**, 215 (2010), arXiv:1012.4484 [hep-lat].
- [9] B. Friman, C. Hohn, J. Knoll, S. Leupold, J. Randrup, *et al.*, Lect.Notes Phys. **814**, 1 (2011).
- [10] theor.jinr.ru/twiki/cgi/view/NICA/NICAWHITEPAPER.
- [11] M. Nahrgang, S. Leupold, C. Herold, and M. Bleicher, Phys.Rev. **C84**, 024912 (2011), arXiv:1105.0622 [nucl-th].
- [12] M. Nahrgang, S. Leupold, and M. Bleicher, Phys.Lett. **B711**, 109 (2012), arXiv:1105.1396 [nucl-th].
- [13] M. Nahrgang, C. Herold, S. Leupold, I. Mishustin, and M. Bleicher, (2011), arXiv:1105.1962 [nucl-th].
- [14] C. Herold, M. Nahrgang, I. Mishustin, and M. Bleicher, Phys.Rev. **C87**, 014907 (2013), arXiv:1301.1214 [nucl-th].
- [15] I. Mishustin and O. Scavennius, Phys.Rev.Lett. **83**, 3134 (1999), arXiv:hep-ph/9804338 [hep-ph].
- [16] K. Paech, H. Stoecker, and A. Dumitru, Phys.Rev. **C68**, 044907 (2003), arXiv:nucl-th/0302013 [nucl-th].
- [17] T. K. Herbst, J. M. Pawłowski, and B.-J. Schaefer, Phys.Lett. **B696**, 58 (2011), arXiv:1008.0081 [hep-ph].
- [18] C. Ratti, M. A. Thaler, and W. Weise, Phys.Rev. **D73**, 014019 (2006), arXiv:hep-ph/0506234 [hep-ph].
- [19] R. D. Pisarski, Phys.Rev. **D62**, 111501 (2000), arXiv:hep-ph/0006205 [hep-ph].
- [20] L. P. Csernai and J. I. Kapusta, Phys.Rev. **D46**, 1379 (1992).
- [21] L. F. Palhares and E. S. Fraga, Phys.Rev. **D82**, 125018 (2010), arXiv:1006.2357 [hep-ph].
- [22] C. Greiner and B. Muller, Phys.Rev. **D55**, 1026 (1997), arXiv:hep-th/9605048 [hep-th].
- [23] D. H. Rischke, Phys.Rev. **C58**, 2331 (1998), arXiv:nucl-th/9806045 [nucl-th].
- [24] T. S. Biro and C. Greiner, Phys.Rev.Lett. **79**, 3138 (1997), arXiv:hep-ph/9704250 [hep-ph].
- [25] T. Kahara and K. Tuominen, Phys.Rev. **D78**, 034015 (2008), arXiv:0803.2598 [hep-ph].